SSC-SDE-10

DI
DT

SSC-SDE
SOLENOIDAL DETECTOR NOTES

THE IMPACT OF RESOLUTION, CRACKS AND BEAM HOLES
ON DETECTION OF PROCESSES WITH MISSING ENERGY
SEPTEMBER 1989

R. Michael Barnett, Eric D. Carlson and Ian Hinchliffe

September 1989

SSC-SDE-10
LBL-27797

The Impact of Resolution, Cracks and Beam Holes on Detection of Processes with Missing Energy *

R. Michael Barnett, Eric D. Carlson and Ian Hinchliffe

Physics Division, Lawrence Berkeley Laboratory, Berkeley, CA 94720

Abstract

We have examined detector characteristics which can lead to backgrounds for missing-energy signatures. To do this, we have developed techniques which allow us to look at extremely rare mismeasurement of jets in high-rate QCD multi-jet processes. We believe that mismeasurement (smearing) can be effectively handled even if resolution is relatively poor, cracks exist, and there are non-Gaussian tails. We also discuss the η coverage (and resolution at large $|\eta|$) required to restrict backgrounds to a level that allow detection of this missing-energy signature.

*This work was supported by the Director, Office of Energy Research, Office of High Energy and Nuclear Physics, Division of High Energy Physics of the U. S. Department of Energy under Contract DE-AC03-76SF00098, and by the National Science Foundation under grant PHY-86-15529.

Multi-jet final states where the jets have transverse energy of order 100 GeV occur copiously at the SSC[1]. If we are interested in some new physics process that gives rise to jets and missing transverse energy, we must consider the small probability that a mismeasurement of the multijet final state will give rise to an event that appears to have missing-transverse energy. Similarly, if the calorimetry on an SSC detector covers the region out to $|\eta| = 4.5$-5.0 (about 1 degree or less), it is quite improbable that a jet will escape through the small beam hole and yet have 100 GeV of transverse energy (this would require a multi-TeV jet). But this small probability coupled to the large jet rate can lead to appreciable backgrounds to missing transverse energy signatures.

These "detector" backgrounds to missing transverse momentum signatures should not be examined outside the context of physical processes. Here we will be concerned with a large signal coming from pair production of gluinos[2], one of which decays directly to a photino (leading to missing transverse energy) and a quark-antiquark pair. The other gluino decays to quark-antiquark, quark-antiquark and a photino. This process which we assume has an overall branching fraction[3] of about 10% can give rise to a final state of up to 6 jets and missing transverse momentum carried off by the photinos. The exact number of jets depends upon the jet definition. Here we shall define a jet to be a parton with transverse momentum greater that 50 GeV and a separation from other partons of $\Delta R = \sqrt{((\Delta\eta)^2 + (\Delta\phi)^2)} > 0.7$. Some of these partons from the gluino decays are lost or merged together by this criterion. Figure 1 shows the cross section as a function of missing transverse energy and illustrates that, with this jet definition, the final state with the largest rate has three jets in it. The signal that we therefore consider is three jets and missing E_T. We expect that the conclusions reached will also be valid for final states with two or four jets. Since the gluinos are produced dominantly by gluon-gluon annihilation, the cross-section for this process is large and any detector that is reasonably hermetic should be able to extract a signal. Although the production cross section for light gluinos is large, the missing E_T is small and the backgrounds due to detector inadequacies are more serious than for heavy gluinos. We therefore consider a mass of 250 GeV in this note. (In a later note[4], we will consider the detector requirements from a study of a rare process with missing energy, *i.e.* Higgs decay to ZZ with one $Z \to \nu\bar{\nu}$ and the other $Z \to e^+e^-$.)

Our goal in detector design should not be to reduce any detector backgrounds to some minimal level but only to less than physics backgrounds. The physics background we consider here is the production of a Z boson and 3 jets[5] (where $Z \to \nu\bar{\nu}$). There are other possible backgrounds such as the production of a W and three jets followed by the decay of the W to $\tau\nu$ or the production of $t\bar{t}+$ *jets* where the t decays hadronically and the $\bar{t}$ decays to $\bar{b}\tau\nu$ or *vice versa.*

The design of SSC detectors requires an understanding of the impact of resolution, cracks and rapidity coverage on detection of physical processes. However, the relative rarity of events with large missing E_T creates problems for Monte Carlo simulations of such processes, since huge numbers of events need to be generated in order to have sufficient statistics in the small fraction of background events with large missing energy. In this note we discuss techniques we have developed to obtain high statistics in the region $E_T(missing) =$ 100-200 GeV.

The work described here was performed with the Monte Carlo program Papageno[6], which is an iterative parton Monte Carlo. The phase space integration is done using VEGAS[7], which adjusts the integration grid to concentrate points in the regions where the product of the phase space weight and the squared matrix element is largest. In order to simulate the effects of detector resolution, each jet's momentum, p, is smeared by choosing a mismeasurement, Δp, according to a Gaussian distribution (with no weight factor):

$$P_g(\Delta p) = \frac{1}{\sigma\sqrt{2\pi}} e^{-(\Delta p)^2/2\sigma^2}.$$

In order to enhance the mismeasurement signal for $E_T(missing) > 100$ GeV, we used a combination of two techniques. First we generate more events in the tail of the Gaussian distribution by generating the distribution in Δp according to

$$P_b(\Delta p) = \frac{1}{\sigma\pi\sqrt{2}} \frac{1}{(1 + \frac{(\Delta p)^2}{2\sigma^2})},$$

and then in the distributions multiplied each event's weight by P_g/P_b. However, this reweighting was only done at the time of histogramming and not in the weight given to VEGAS since this random weight factor could only confuse the integration method used by VEGAS. (Two final states with identical parton momenta and therefore identical cross-section end up with different probabilities after the momentum smearing.) The advantage of this method is that roughly $1/n$ of the events have $\Delta p > n\sigma$. Even this technique is inadequate to obtain good statistics at large $E_T(missing)$ since most events are generated with small $\hat{s}$ (total center of mass energy squared of the parton collision). To handle this problem we take advantage of the iterative nature of integration routine VEGAS (in Papageno). We multiply the weight received by VEGAS by $\hat{s}^5$ but then divide the weight by that same factor before creating our distributions. This causes VEGAS to make a denser grid of points at larger $\hat{s}$. The final result of this combined technique is that the bin-to-bin fluctuations at $E_T(missing)$ of 100-200 GeV are as good as at very low $E_T(missing)$. The actual power of $\hat{s}$ chosen will vary depending upon the process and detector resolution.

For studies of the problem of jets escaping down the beam hole, the statistics are less sensitive to the power of $\hat{s}$ multiplied times the VEGAS weight (we used $\hat{s}^2$), since this process does not require such large $\hat{s}$.

The particular problems we investigated here involved the signature of three jets with $E_T(jet) > 50$ GeV (if there was a fourth jet with 50 GeV or more, the event was rejected). No other cuts were made initially. Under these conditions the physics background $Z(\rightarrow \nu\bar{\nu})$ plus 3 jets is at least a factor of 5 smaller than the signal for $E_T(missing)$ below 200 GeV (see Figure 2).

We report here on the results of various studies in which we used the following form for the resolution:

$$\frac{\sigma}{p} = \frac{B}{\sqrt{E}} + C$$

where we chose $B = 0.4$ or 0.8 and $C = 0$ or 0.015. To account for cracks which degrade resolution we chose what may be a worst case scenario. We chose two cracks centered at $|\eta| = 1.775$ and at 3.025. The factor B above was modified such that $B \rightarrow B + 0.7$ at $|\eta| = 1.775$ and 3.025, and fell linearly to the original B at a distance of 0.125 (in η) on either side of the center position. The resolution peak at $|\eta| = 1.775$ is similar to that shown in the a recent study of detector hermeticity[8]. Since we use a parton Monte Carlo, a "jet" is either completely in the crack or completely out (so we may exaggerate the effects of cracks).

The final resolution effect we considered was the possible existence of non-Gaussian tails. The CDF collaboration at the Tevatron Collider has seen no evidence of such tails[9] in the region away from cracks, but the SSC will have much higher luminosity and jets with much higher E_T. To mock this effect, we have added a second wider Gaussian on top of the original Gaussian; this second Gaussian was taken to have a resolution (σ) 3 times that of the original and 5% the magnitude of the original. Anything much larger would probably be inconsistent with the CDF results.

We can produce missing-energy Monte Carlo events by generating 3-jet events and smearing their momenta. Alternatively, we generate 4-jet events and smear momenta so that one jet fluctuates below the 50 GeV threshold. However, we find that missing E_T from four-jet events is dominated by the case where one jet is lost down the beam hole (see below). We first discuss the smearing effects from the 3-jet events. In Fig. 2 we show the results without the added tails, with $C = 0$, with $B = 0.4$ and 0.8, and with the two cracks included. In either case, the physics background (Z plus 3 jets) would dominate these detector backgrounds for $E_T(missing) > 100$ GeV. In Fig. 3 we examine the most extreme case in which we have added the mockup of the non-Gaussian tails, taken $C = 0.015$ and $B = 0.8$, and included the two cracks at $|\eta| = 1.775$ and 3.025. The results are represented by the highest histogram, and clearly this background would dominate the signal if no further cuts were made. We will return to the subject of additional cuts after discussing the impact of beam holes.

If a jet is produced with several TeV and escapes down the beam hole, then it is possible that it has $E_T > 100$ GeV, which will be observed as missing energy. Since we require 3 energetic observed jets, we must generate these events with 4 initial jets. We found that the beam-hole effects dominated the smearing effects for 4-jet events, and since the smearing technique degrades our statistics in this case, we have examined the beam-hole losses without smearing. In Fig. 4 we see that a beam hole at $|\eta| > 5.0$ causes no problems above $E_T(missing)$ of 100 GeV. However, the beam hole at $|\eta| > 4.5$ would lead to a background which is comparable to the signal in the 100-200 GeV region of $E_T(missing)$ if no additional cuts are made. Note, however, that the effects have been exaggerated because our "jets" (partons) are either entirely in the beam hole or entirely in the detector.

We have examined a variety of distributions from the 3- and 4-jet backgrounds and from the gluino pair production signal to find the appropriate variables in which to apply cuts in an attempt to reduce the background. One of these variables (call it M_g) is the invariant mass of the two leading jets together with the transverse missing momentum vector; this is an attempt to find the mass of the gluino since the two leading jets are likely to have come from the gluino that decayed to quark, antiquark and photino. For smearing, our worst case scenario was the one with the non-Gaussian tails. We find that a variety of mass and energy variables show significantly harder distributions for the background than for the signal (these include $\Sigma E_T(scalar)$, E_T of the leading and second jets, M_g, and the invariant mass of the 3 jets). Since these probably depend on the mass of the gluino chosen, we do not make use of them.

Other variables which can separate signal and background even more effectively include the difference in the azimuthal angles of the missing momentum and the nearest jet, the difference in the azimuthal angles between the two leading jets and the circularity. Circularity is defined as $C = \frac{1}{2}\min(\Sigma \widehat{E_T} \cdot \hat{n})^2/(\Sigma \left|\widehat{E_T}\right|^2)$ where $\widehat{E_T}$ is the two-dimensional vector describing the components of the jet's momentum in a plane transverse to the beam and $\hat{n}$ is a unit vector in that plane. The sum is over jets and the minimization is over all possible values of $\hat{n}$; $C = 0$ is pencil-like and $C = 1$ is isotropic. We show these variables in Figs. 5-7. In Fig. 3 we show the impact on the $E_T(missing)$ distribution of making cuts in the angle between the missing momentum and the nearest jet. It shows that, even in this worst case, resolutions and cracks are not a problem if a single cut is made.

In the approximations we are using (*i.e.*– jets are partons, and only 3-jet events considered), there is a variable which can eliminate *every* background event from mismeasurement. This is the sum of the azimuthal angles between each pair of the three leading jets. This variable measures whether or not the three leading jets lie within one hemisphere (in which case the sum is less than 360°); any event with jets not within a hemisphere adds to 360° exactly. With only 3-jets generated for the background, clearly the sum will always be 360° whereas less than half the signal is at 360°. In a more realistic world with more than 3 jets, there presumably will remain a substantial difference between signal and background, but we have not pursued this question since other variables reduce the background sufficiently.

Returning to the beam-hole problem, we find that distributions such as $\Sigma E_T(scalar)$, E_T of the leading, second and third jets, and the invariant mass of the 3 jets are virtually identical for signal and background. Variables that were effective against the smearing background are often not useful here; the azimuthal angle distributions and the circularity look very similar for signal and background. Another variable, p_T^{out}, the missing transverse momentum out of the plane defined by the beam and the highest E_T jet, does not distinguish the signal from either of these types of backgrounds.

However, the variable, M_g, described above (which attempts to find the mass of the gluino) is significantly different as shown in Fig. 8. By requiring $M_g < 300$ GeV we greatly reduce the background as in Fig. 9 (the signal is also slightly reduced, but on the scale of this figure the difference looks small). Another variable which we could make use of is the rapidity of the vector sum of the three leading jets. Since the jet which escapes the beam hole has extremely high momentum, we expect the other jets to tend to balance it, and this is the case as shown in Fig. 10.

In summary, we have considered here the missing-energy signal from a high-rate process, but it is a process with modest $E_T(missing)$. We have developed new techniques which allow us to look at rare events with badly mismeasured jet momenta and obtain extremely good statistics at very large $E_T(missing)$. We find that the background due to smearing is important only in the case where the resolution is poor and there exist important non-Gaussian tails. Even in this case it is easy to make simple cuts which will remove most of this background in the $E_T(missing) > 100$ GeV region. We conclude that excellent resolution is not required, and that cracks which significantly degrade resolution in a limited rapidity region are of no concern for this process.

The problem of events with an extremely energetic jet escaping through the beam hole and giving significant $E_T(missing)$ can be more serious. We found that coverage out to $|\eta| = 5.0$ would keep this background to manageable levels, but that coverage out to $|\eta| = 4.5$ might result in a large background. There are cuts that may bring the background rate down to manageable levels, but a safer approach would be to have some calorimetry out to $|\eta| = 5.0$ so that some or all of the energetic jets near the beam hole can be detected. Certainly there is no need for good resolution in the high $|\eta|$ region, since the only need is to veto against events with extremely high energy jets.

In conclusion, we feel that this missing energy process is not very demanding on the detector in the SSC environment. A separate note will look at a rare process with larger missing energy.

Acknowledgment

This work was supported by the Director, Office of Energy Research, Office of High Energy and Nuclear Physics, Division of High Energy Physics of the U.S. Department of Energy under Contract DE-AC03-76SF00098. Accordingly, the U.S. Government retains a nonexclusive, royalty-free license to publish or reproduce the published form of this contribution, or allow others to do so, for U.S. Government purposes.

References

[1] E. Eichten *et al.*, *Rev. Mod. Phys.* **56**, 579 (1984).

[2] For a review see, for example, I Hinchliffe, *Ann. Rev. Nucl. and Part. Sci.* **36**, 505 (1986). For earlier work on supersymmetric signals at SSC, see R. M. Barnett *et al.*, in *Proc. 1988 Snowmass Summer Study* Ed. S. Jensen, World Scientific publishing (1989).

[3] R. M. Barnett, J.F. Gunion and H.E. Haber, *Phys. Rev.* **D37**, 1892 (1988).

[4] R. M. Barnett and I. Hinchliffe, in preparation.

[5] K. Hagiwara and D. Zeppenfeld *Nucl. Phys.* **B363**, 560 (1989).

[6] PAPAGENO, I. Hinchliffe, in preparation.

[7] G.P. Lepage, *J. Comput. Phys.* *27, 192 (1978).*

[8] M. Strovink, W. Wormersley and G. Forden, "Hermeticity in Three Calorimetric Geometries", Workshop on Calorimetry, U. of Alabama, 13-17 March 1989.

[9] J. Huth, FNAL-CONF 89/117E.

Figure 1

The missing transverse energy distributions resulting from gluino pair production for a gluino mass of 250 GeV. The lines are labelled by the number of jets in the event. The curve marked "all" is the total rate, *i.e.* the sum of the other curves.

Figure 2

The missing transverse energy distributions resulting from gluino pair production (solid curve), $Z(\rightarrow \nu\bar{\nu})$ plus 3 jets (dash-dotted curve), and 3 mismeasured jets (QCD) where resolution is $0.4/\sqrt{E}$ (solid histogram), $0.8/\sqrt{E}$ (dashed histogram) and the cracks described in the text are included.

Figure 3

The missing transverse energy distributions resulting from gluino pair production (solid curve), $Z(\rightarrow \nu\bar{\nu})$ plus 3 jets (dash-dotted curve), and 3 mismeasured jets (QCD) where resolution is $0.8/\sqrt{E} + 0.015$ (dotted histogram) with the cracks and with the non-Gaussian tails described in the text included. The solid and dashed histograms are also 3-jet QCD events but have cuts of $> 20°$ and $> 40°$ respectively on the azimuthal angle between the missing transverse momentum and the nearest jet (of the three jets with the highest E_T).

Figure 4

The missing transverse energy distributions resulting from gluino pair production (solid curve), $Z(\rightarrow \nu\bar{\nu})$ plus 3 jets (dash-dotted curve), and 4-jet (QCD) events in which one jet escapes though the beam hole at $|\eta| = 4.5$ (dashed histogram) and $|\eta| = 5.0$ (solid histogram).

Figure 5

The distribution at $E_T(missing) > 100$ GeV of the azimuthal angle between the missing transverse momentum and the nearest of the three jets with the highest E_T. The dashed curve results from gluino pair production. The solid histogram results from three mismeasured jets (QCD) where resolution is $0.8/\sqrt{E}+0.015$ (dotted histogram) with the cracks and with the non-Gaussian tails described in the text included. The normalization of the solid histogram has been adjusted to facilitate comparison.

Figure 6

The distribution at $E_T(missing) > 100$ GeV of the azimuthal angle between the two jets with the highest E_T. The dashed curve results from gluino pair production. The solid histogram results from three mismeasured jets (QCD) where resolution is $0.8/\sqrt{E} + 0.015$ (dotted histogram) with the cracks and with the non-Gaussian tails described in the text included. The normalization of the solid histogram has been adjusted to facilitate comparison.

Figure 7

The distribution at $E_T(missing) > 100$ GeV of the circularity (defined in the text). The dashed curve results from gluino pair production. The solid histogram results from three mismeasured jets (QCD) where resolution is $0.8/\sqrt{E} + 0.015$ (dotted histogram) with the cracks and with the non-Gaussian tails described in the text included. The normalization of the solid histogram has been adjusted to facilitate comparison.

Figure 8

The distribution at $E_T(missing) > 100$ GeV of the invariant mass, M_g, of the missing transverse momentum and the two nearest of the three 50 GeV jets (this variable tries to find the gluino mass). The dashed curve results from gluino pair production. The solid histogram results from four-jet (QCD) events in which one energetic jet escapes the beam hole at $|\eta| = 4.5$. The normalization of the solid histogram has been adjusted to facilitate comparison.

Figure 9

The missing transverse energy distributions resulting from gluino pair production (solid curve), $Z(\to \nu\bar{\nu})$ plus 3 jets (dash-dotted curve), and 4-jet (QCD) events in which one jet escapes though the beam hole at $|\eta| = 4.5$ (dashed histogram). The solid histogram is also 4-jet QCD events but has had a cut $M_g < 300$ GeV applied (see text for definition).

Figure 10

The distribution at $E_T(missing) > 100$ GeV of the rapidity of the vector sum of the three 50 GeV jets. The dashed curve results from gluino pair production. The solid histogram results from four-jet (QCD) events in which one energetic jet escapes the beam hole at $|\eta| = 4.5$. The normalization of the solid histogram has been adjusted to facilitate comparison.

Figure 1

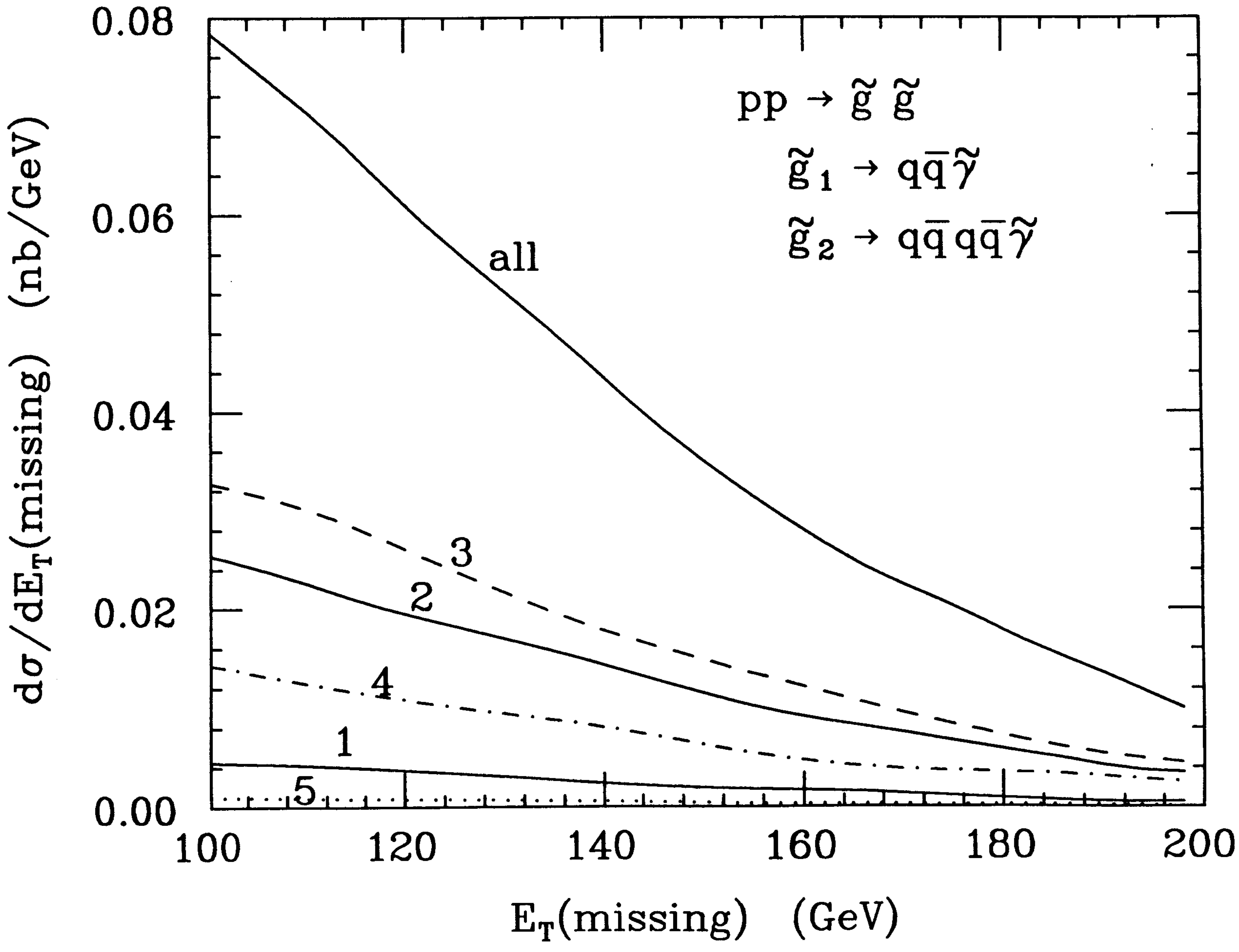

0.08
0.06
0.04
0.02
0.00
100
120
140
160
180
200
$d\sigma/dE_T$(missing) (nb/GeV)
E_T(missing) (GeV)
$pp \to \tilde{g}\,\tilde{g}$
$\tilde{g}_1 \to q\bar{q}\tilde{\gamma}$
$\tilde{g}_2 \to q\bar{q}q\bar{q}\tilde{\gamma}$
all
3
2
4
1
5

Figure 2

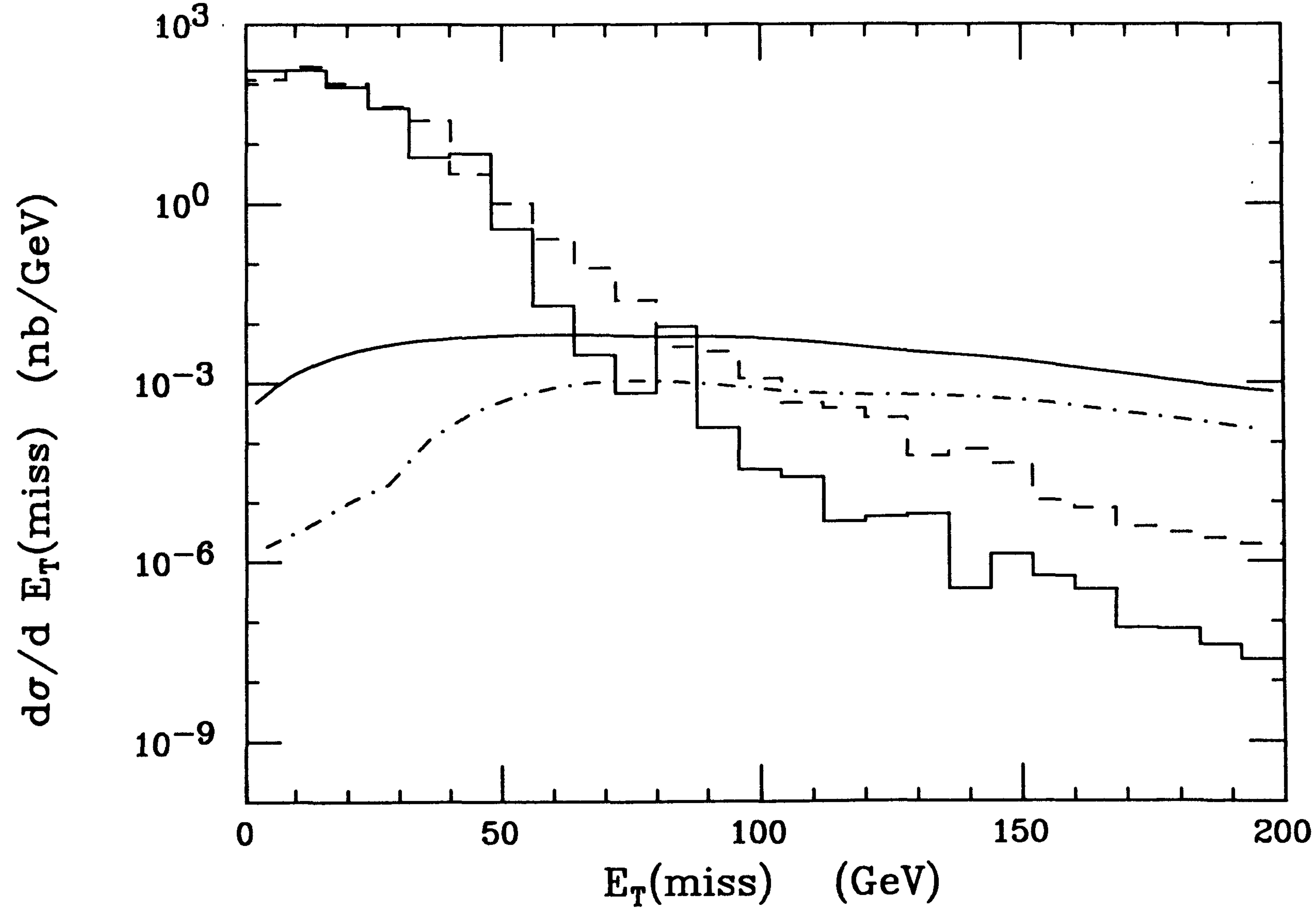

10^3
10^0
10^{-3}
10^{-6}
10^{-9}
0
50
100
150
200
$d\sigma/d\ E_T(\mathrm{miss})$ (nb/GeV)
$E_T(\mathrm{miss})$ (GeV)

Figure 3

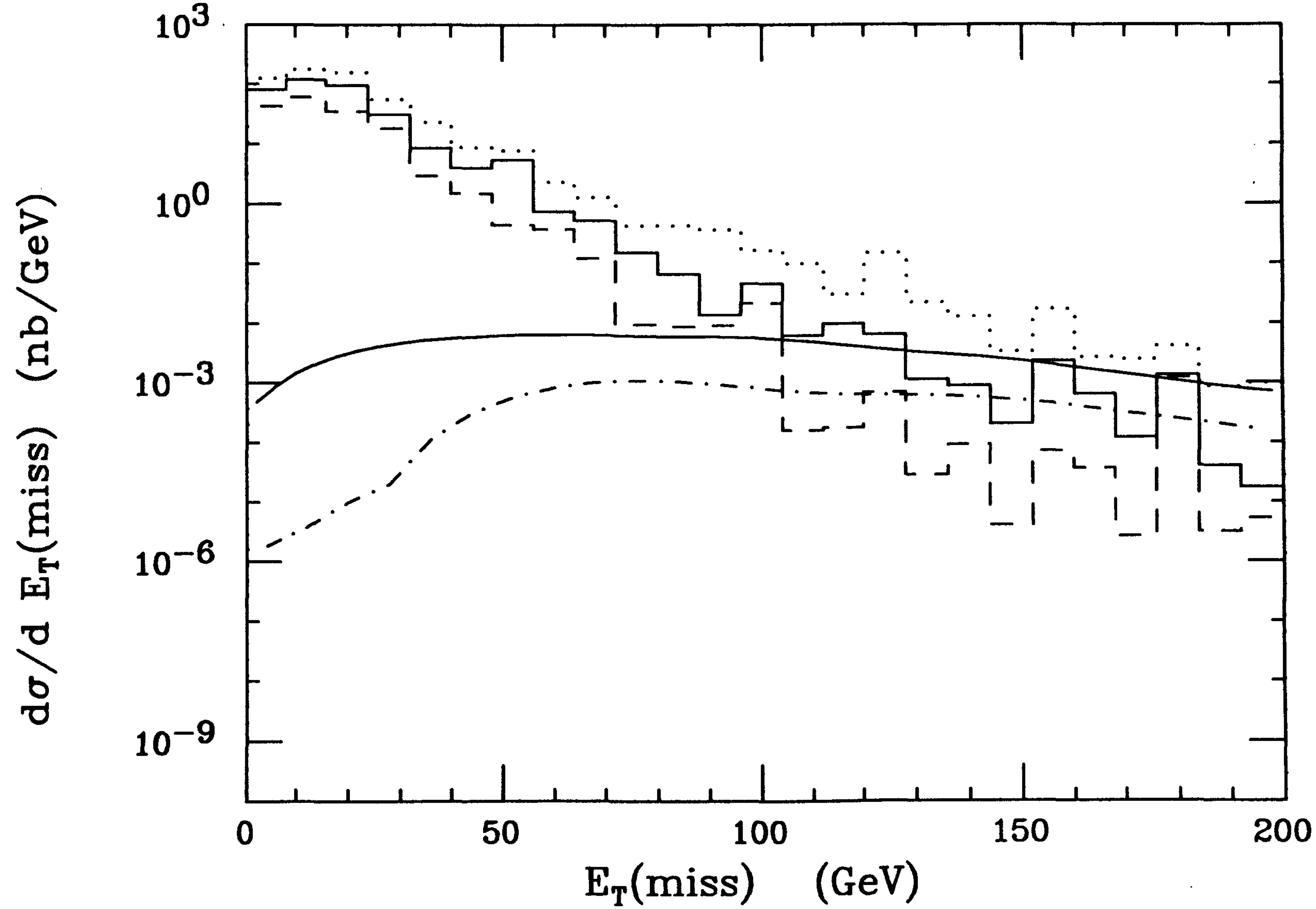

10^{3}
10^{0}
10^{-3}
10^{-6}
10^{-9}
$d\sigma/d\ E_T(\text{miss})$ (nb/GeV)
0
50
100
150
200
$E_T(\text{miss})$ (GeV)

Figure 4

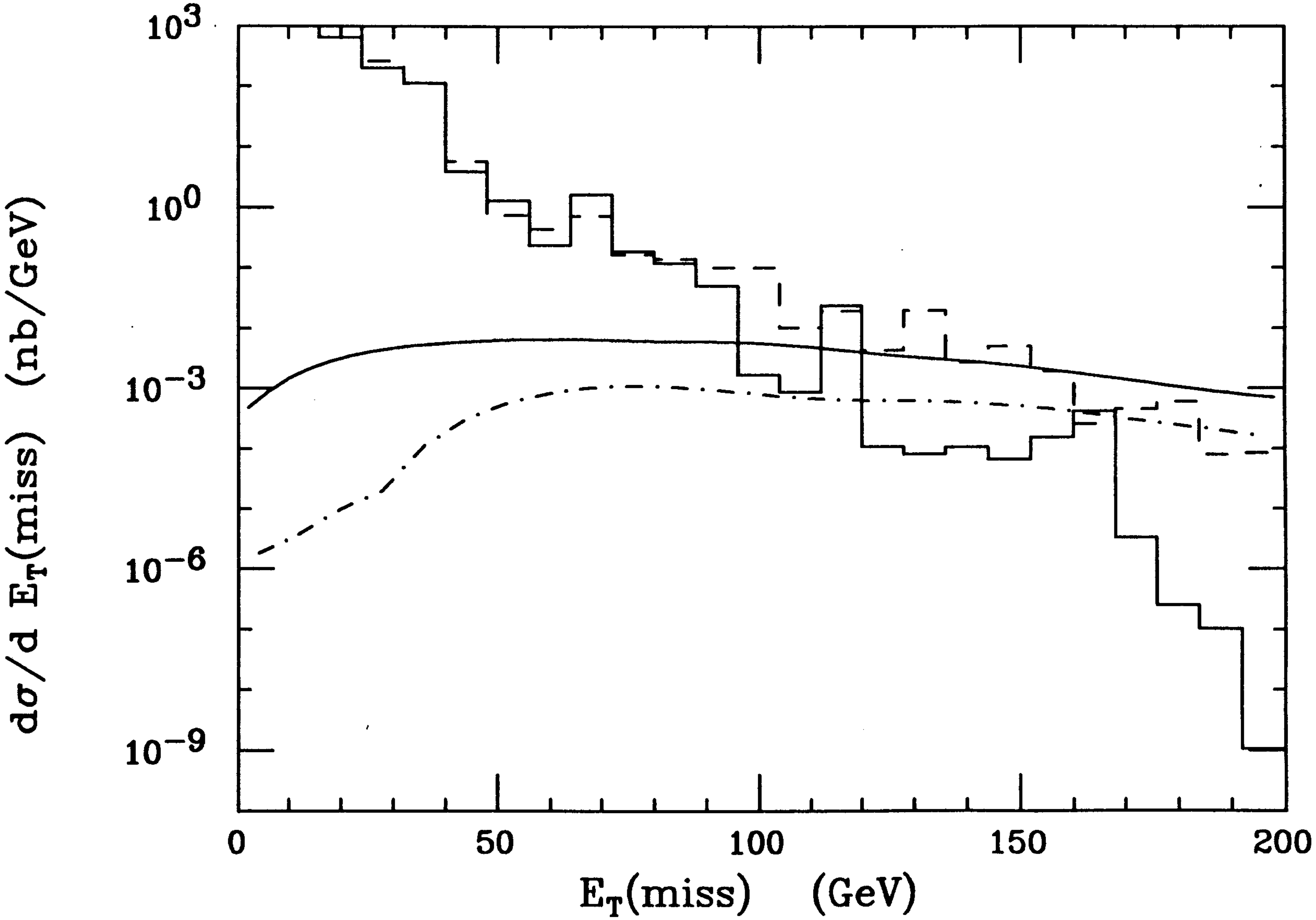

10^3
10^0
10^{-3}
10^{-6}
10^{-9}
0
50
100
150
200
$d\sigma/d\ E_T$(miss) (nb/GeV)
E_T(miss) (GeV)

Figure 5

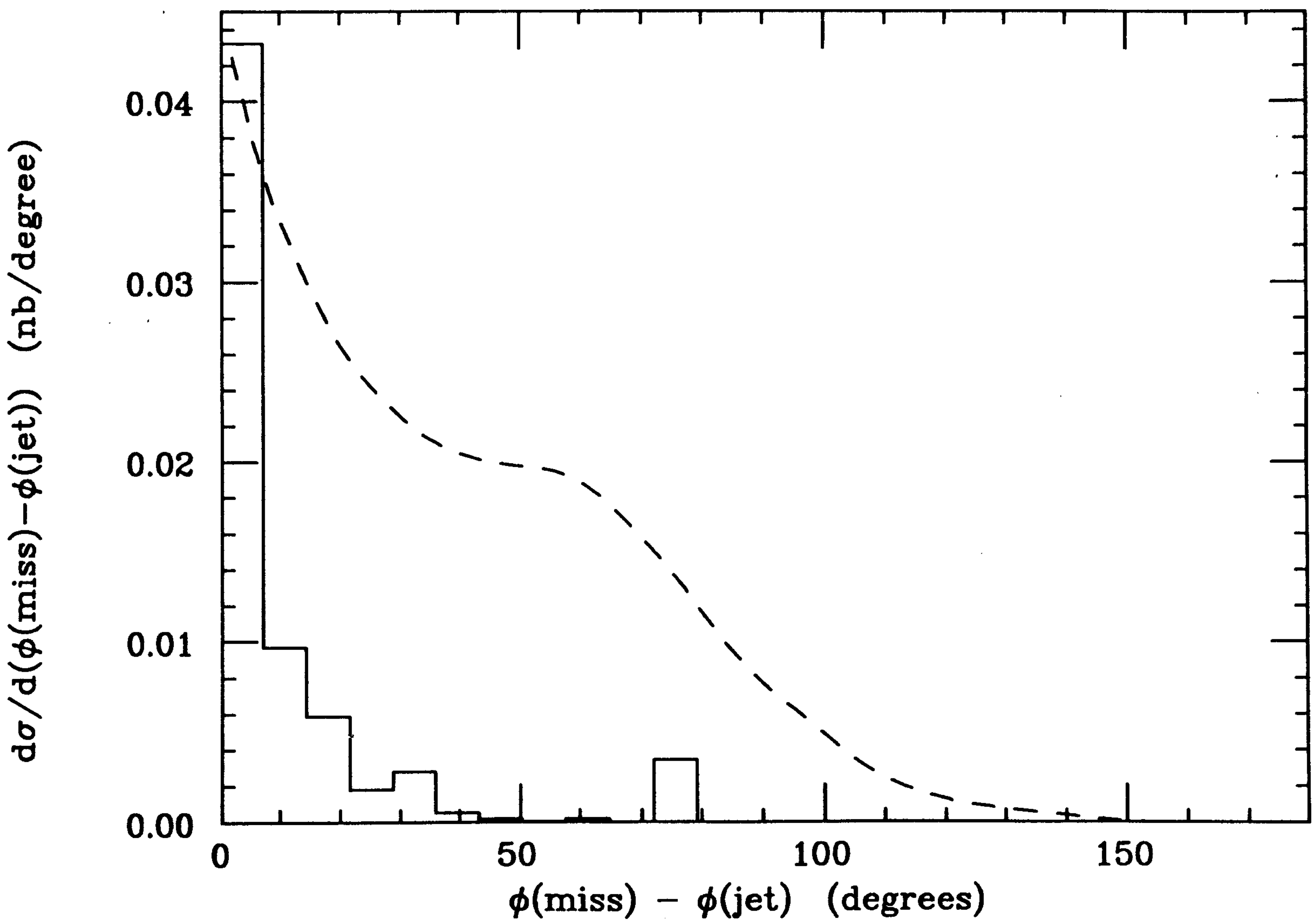

0.04
0.03
0.02
0.01
0.00
0
50
100
150
dσ/d(φ(miss)−φ(jet)) (nb/degree)
φ(miss) − φ(jet) (degrees)

Figure 6

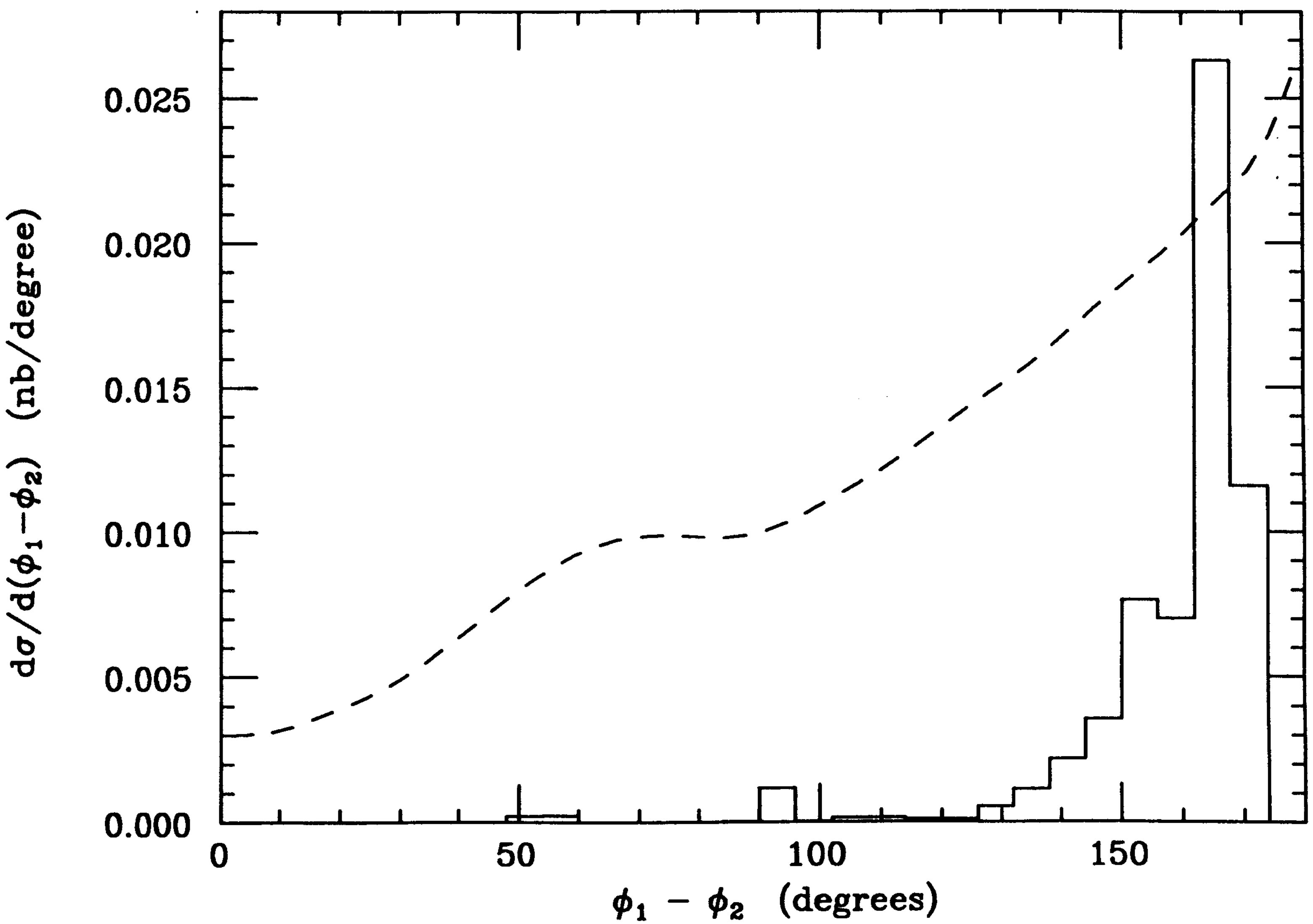
0.025
0.020
0.015
0.010
0.005
0.000
dσ/d(φ1−φ2) (nb/degree)
0
50
100
150
φ1 − φ2 (degrees)

Figure 7

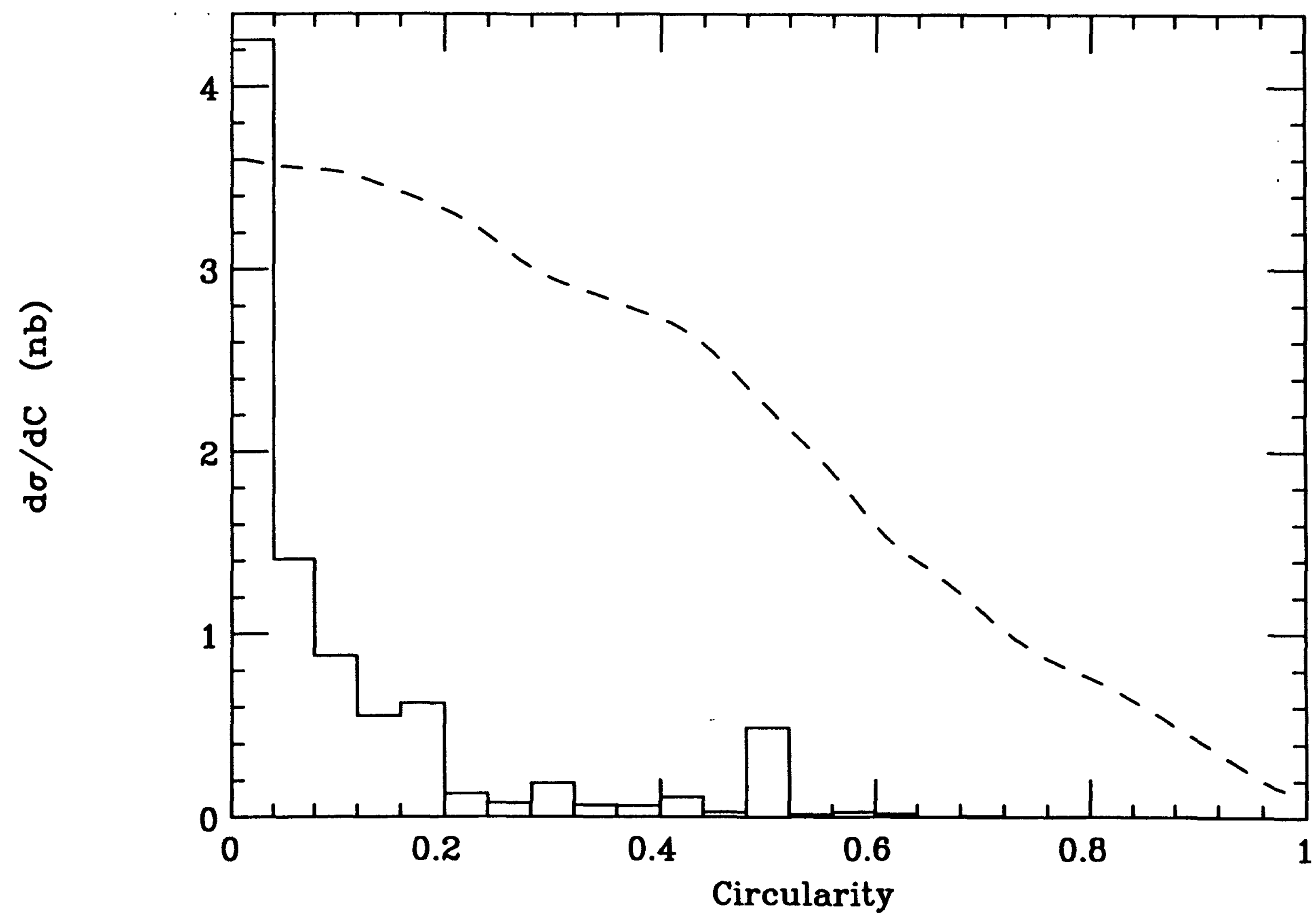

Figure 8

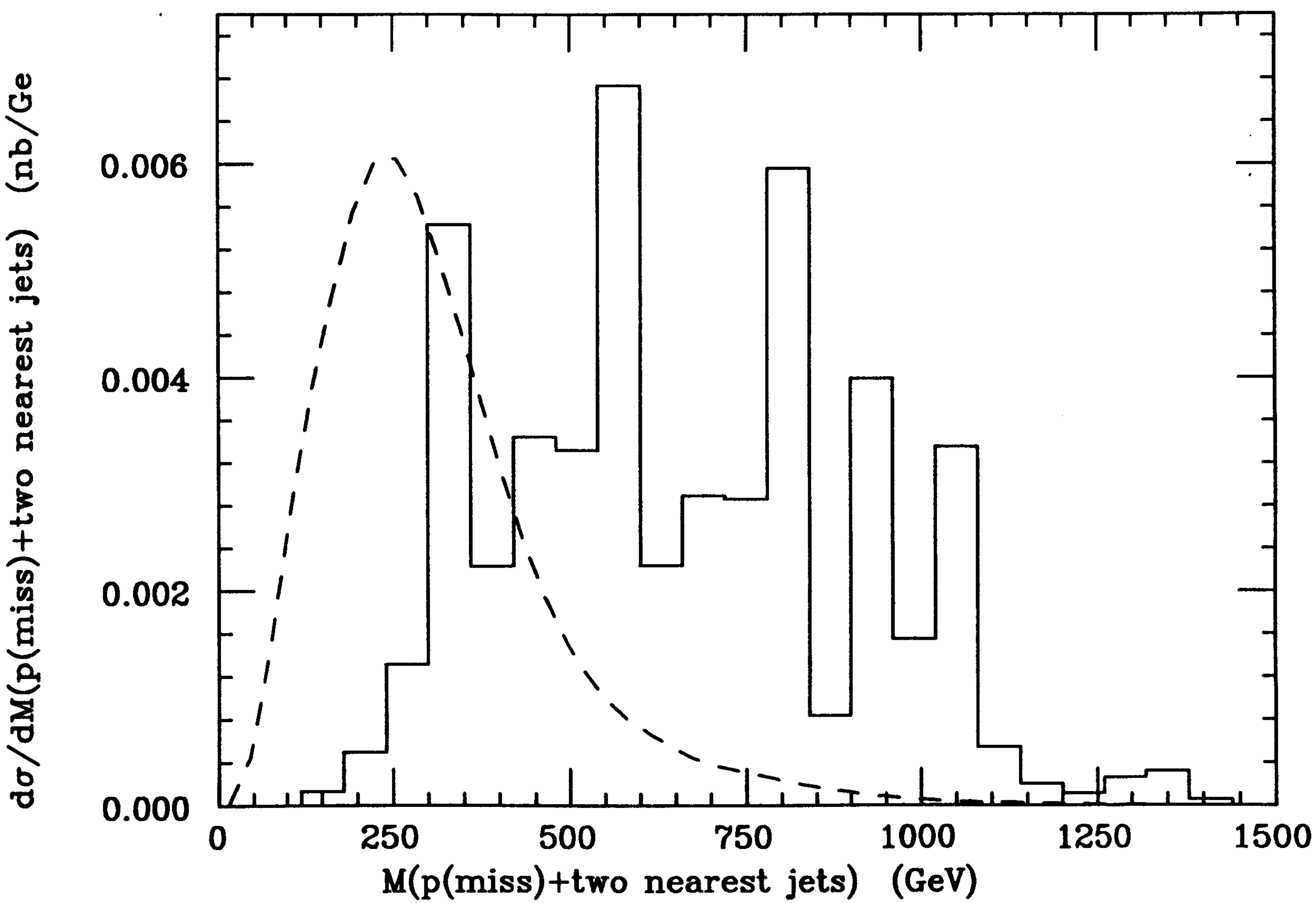

dσ/dM(p(miss)+two nearest jets) (nb/Ge
0.000
0.002
0.004
0.006
0
250
500
750
1000
1250
1500
M(p(miss)+two nearest jets) (GeV)

Figure 9

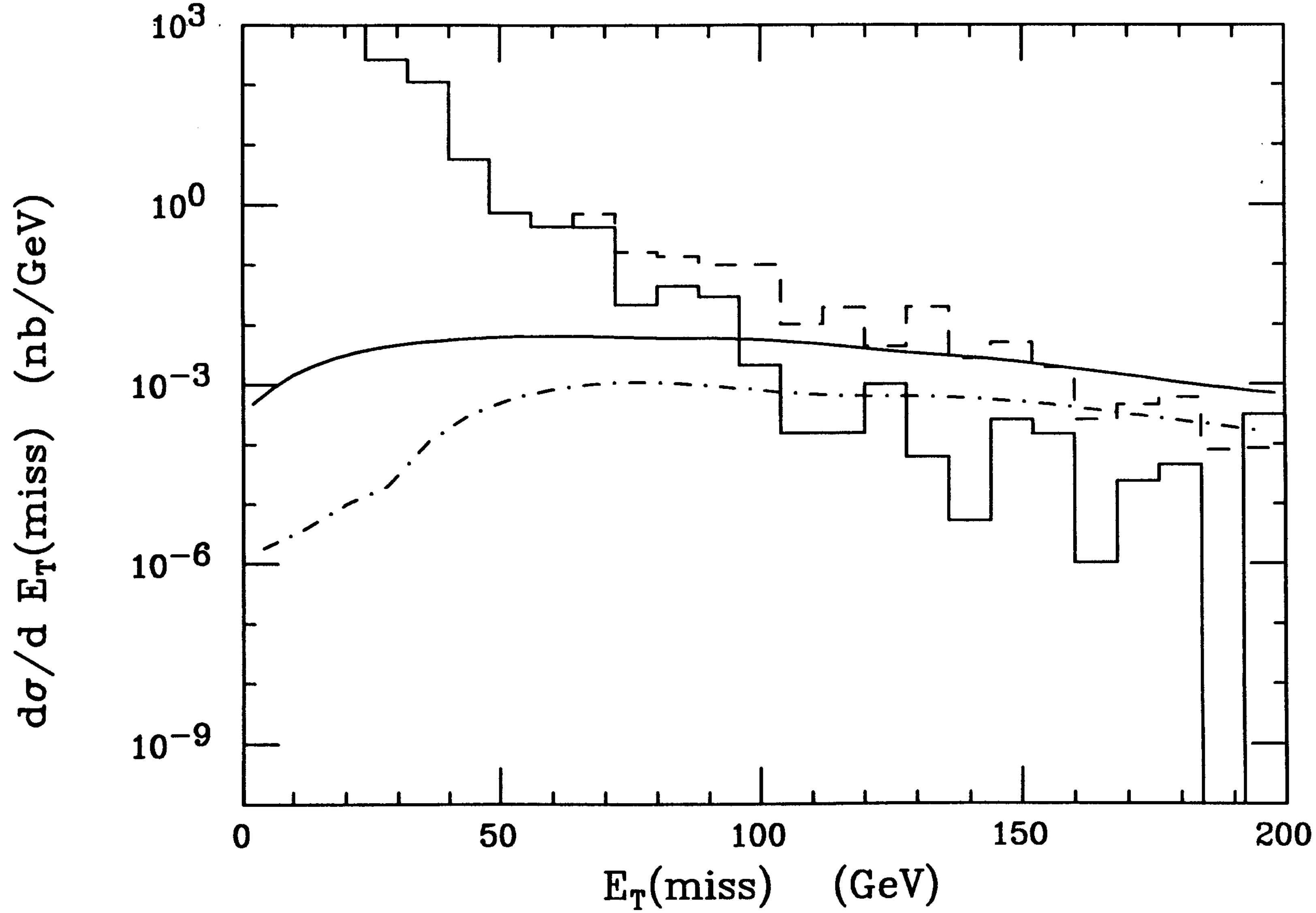

$d\sigma/d\ E_T(\text{miss})$ (nb/GeV)
10^3
10^0
10^{-3}
10^{-6}
10^{-9}
0
50
100
150
200
$E_T(\text{miss})$ (GeV)

Figure 10